Reduced Osteoarthritis Severity in Aged Mice With Deletion of Macrophage Migration Inhibitory Factor

Meredith A. Rowe,[1] Lindsey R. Harper,[2] Margaret A. McNulty,[3] Anthony G. Lau,[4] Cathy S. Carlson,[2] Lin Leng,[5] Richard J. Bucala,[5] Richard A. Miller,[6] and Richard F. Loeser[1]

Objective. **Macrophage migration inhibitory factor (MIF) is a proinflammatory cytokine that is elevated in the serum and synovial fluid of patients with osteoarthritis (OA). This study was undertaken to investigate the potential role of MIF in OA in human joint tissues and in vivo in mice with age-related and surgically induced OA.**

Methods. **MIF in conditioned media from human chondrocytes and meniscal cells and from cartilage explants was measured by enzyme-linked immunosorbent assay. The severity of OA was analyzed histologically in male wild-type and MIF$^{-/-}$ mice at 12 and 22 months of age and following destabilization of the medial meniscus (DMM) surgery in 12-week-old MIF$^{-/-}$ mice as well as in wild-type mice treated with a neutralizing MIF antibody. Synovial hyperplasia was graded in S100A8-immunostained histologic sections. Bone morphometric parameters were measured by micro–computed tomography.**

Results. **Human OA chondrocytes secreted 3-fold higher levels of MIF than normal chondrocytes, while normal and OA meniscal cells produced equivalent amounts. Compared to age- and strain-matched controls, the cartilage, bone, and synovium in older adult mice with MIF deletion were protected against changes of naturally occurring age-related OA. No protection against DMM-induced OA was seen in young adult MIF$^{-/-}$ mice or in wild-type mice treated with anti-MIF. Increased bone density in 8-week-old mice with MIF deletion was not maintained at 12 months.**

Conclusion. **These results demonstrate a differential mechanism in the pathogenesis of naturally occurring age-related OA compared to injury-induced OA. The inhibition of MIF may represent a novel therapeutic target in the reduction of the severity of age-related OA.**

Aging has been well described as a key risk factor for the development of osteoarthritis (OA) (1). While aging does not directly cause OA, aging changes in joint tissues and possibly circulating factors that change with age increase susceptibility to the development of the disease. Aging changes are reflected in the cartilage matrix, including thinning of the articular cartilage (2) and the accumulation of advanced glycation end products, which alters the biomechanical properties of the joint (3). Aging changes are also evident in chondrocytes, where chondrocytes isolated from older individuals are more resistant to stimulation with the growth factors insulin-like growth factor 1 (4,5), transforming growth factor β (6), and bone morphogenetic protein 6 (7) than chondrocytes isolated from younger individuals. Inflammatory mediators have been found to be up-regulated in aged joint tissues, including interleukin-7 (IL-7) in chondrocytes and synovial fluid in humans and IL-33, CXCL13, CCL8, and CCL5 in the mouse knee joint (for review, see ref. 8). The increased expression of these inflammatory mediators, which is compounded by aging changes in the tissues, may contribute to the development of OA.

Macrophage migration inhibitory factor (MIF) is an inflammatory cytokine that has been studied for its role in

the immune system. MIF has been shown to function as a cytokine that signals through the CD74 receptor (9) to increase neutrophil migration to regions of inflammation and to promote the innate immune response (10,11). Additionally, MIF promotes macrophage activation, increasing phagocytosis and destruction of pathogens (11,12). MIF has been studied in autoimmune diseases including rheumatoid arthritis (RA) and systemic lupus erythematosus (SLE). It has been shown to promote matrix metalloproteinase 1 (MMP-1) and MMP-3 production in synovial fibroblasts isolated from the knee joints of RA patients (13) and also has been shown to be significantly elevated in RA synovial fluid (14). In a more recent study, inhibition of MIF function either by deletion of MIF, or its receptor, CD74, was found to reduce the severity of disease in an RA model by reducing both inflammation and bone erosion (15). In SLE, the amount of MIF in serum is positively correlated with tissue damage (16), and the renal expression of MIF was shown to be significantly elevated in an SLE-prone mouse model (17). The level of MIF was noted to be elevated in the serum and synovial fluid of patients with knee OA compared to healthy controls (14,18). However, the potential contribution of MIF to the development of OA has not been studied previously.

Recently, MIF$^{-/-}$ 129Sv/C57BL/6 mice were reported to have an increased lifespan compared to wild-type controls, suggesting a role for MIF in the aging process (19), although more recent data suggest that this beneficial effect may be absent on other genetic backgrounds (Miller RA: unpublished observations). Like OA, atherosclerosis is a common disease of aging, and inhibition of MIF has been found to reduce atherosclerosis in a mouse model of the disease (20), suggesting that MIF may represent a therapeutic target for age-related disease. Given the association between aging and OA, we sought to determine the contribution of MIF to the development of OA. We found that genetic disruption of MIF decreased the severity of naturally occurring OA in aged mice but not in a surgically induced model of OA in younger adult mice.

MATERIALS AND METHODS

Chondrocyte and meniscal cell isolation and culture. Normal human donor tissue (from both knee and ankle joints) was obtained from the Gift of Hope Organ and Tissue Donor Network (Elmhurst, IL) through the Rush University Medical Center in Chicago, IL. Osteoarthritic tissue was obtained as surgical waste from total knee replacement surgeries performed in the Department of Orthopaedic Surgery at Wake Forest Baptist Health and at the University of North Carolina Hospitals. The use of human tissue was approved by the institutional review boards at Rush University, Wake Forest Baptist Health, and the University of North Carolina at Chapel Hill. All human donor tissue was de-identified before receipt,

and the cartilage and meniscus were processed separately. The cartilage was dissected away from the subchondral bone in small flakes and rinsed in serum-free Dulbecco's modified Eagle's medium (DMEM)/F-12 media (Gibco Life Technologies) to prevent the tissue from drying out. After the excess fat and ligamentous tissue were removed, the meniscus was dissected into small pieces to enable more efficient digestion. Cells were isolated separately from cartilage and meniscus using Pronase and collagenase digestion as previously described (21). The cells were cultured in 10% serum DMEM/F-12 media until confluent. Cultures were serum starved overnight before media collection.

A 4-mm biopsy punch was used to harvest human cartilage explants from the cartilage pieces that had been dissected away from the subchondral bone. Three explants per donor were pooled in 1 well and cultured in 10% serum DMEM/F-12 media for ~72 hours. The explants were serum starved for 48 hours before media collection. The explants were digested in papain, and the DNA content was quantified using a PicoGreen kit (Life Technologies) as previously described (22).

Experimental animals. The mice used for these studies were housed and maintained according to the Institutional Animal Care and Use Committee guidelines at the respective institutions where each study was performed (The University of Michigan, Wake Forest School of Medicine, and The University of North Carolina at Chapel Hill). Knee joints from MIF$^{-/-}$ and wild-type mice for the aging experiment were from a previously published study (19). For the surgically induced OA experiments, the MIF$^{-/-}$ mouse colony was bred on the 129Sv/C57BL/6 mixed background. The colony was maintained by heterozygous breeding, so the MIF$^{-/-}$ and wild-type mice used in this study were age- and strain-matched littermates. The C57BL/6 mice used in the neutralizing antibody experiment were purchased directly from The Jackson Laboratory.

Enzyme-linked immunosorbent assay (ELISA). MIF content in serum-free conditioned media was quantified by solid-phase ELISA (R&D Systems) according to the manufacturer's protocol. Due to the high level of MIF in the media, the media samples were diluted 1:25 in the assay.

MIF immunostaining. Normal and OA human cartilage sections were a kind gift from Dr. Martin Lotz (Scripps Research Institute, La Jolla, CA). Human cartilage sections and mid-coronal sections from 12-month-old wild-type and MIF$^{-/-}$ mouse knee joints were immunostained with anti-MIF (Life Technologies). Sections were deparaffinized and rehydrated in serial ethanol washes followed by antigen retrieval in citrate buffer. Sections were first blocked with 3% H$_2$O$_2$ (Fisher Scientific) and then with Protein Block (Dako). The primary antibody was diluted in antibody diluent (Dako) and incubated on the sections overnight at 4°C. The following day, the sections were incubated with horseradish peroxidase–linked secondary antibody (Dako) and developed with the diaminobenzidine chromogen (Dako). The sections were counterstained in Mayer's hematoxylin (Sigma) and then dehydrated in serial ethanol washes.

Destabilization of the medial meniscus (DMM) procedure. DMM was performed in 12-week-old male MIF$^{-/-}$ and wild-type mice as previously described (23). This procedure induces OA by transecting the medial meniscotibial ligament. For the sham surgery, the joint was opened and visualized, but the medial meniscotibial ligament was not cut. We randomly assigned 14–16 mice to each surgical group and to each of the anti-MIF treatment and control groups (described below).

The number of mice chosen for the present study was based on a power calculation using data from a previously published DMM and sham surgery control experiment from our group that included 12-week-old male C57BL/6 mice (23) and found that a sample size of 12 mice per group would provide >80% power to detect at least a 50% difference in articular cartilage structure (ACS) scores between groups. After the surgical procedure, the mice were monitored closely for signs of apparent pain or adverse effects of the procedure. The mice were maintained in normal housing conditions and allowed to exercise through normal activities. Ten weeks after surgery, mice were euthanized and the hind limbs were collected in 10% formalin (Fisher Scientific) for histologic analysis.

In the anti-MIF experiment, a neutralizing murine anti-MIF IgG1 (clone NIHIIID.9) and isotype control antibody were purified from ascites fluid using Protein A/G spin columns (Thermo Scientific). Following isolation, the antibodies were dialyzed overnight in Dulbecco's phosphate buffered saline (Lonza) and then filter-concentrated by centrifugation (Millipore). The antibody concentration was measured by bicinchoninic acid assay (Thermo Scientific). After DMM surgery, mice were allowed to recover for 5 days before antibody treatment began. The antibodies were administered by intraperitoneal injection for the duration of the study at a dosage (20 mg/kg twice per week) previously shown to neutralize MIF in vivo (24). The mice were euthanized 10 weeks after surgery, and legs were collected in formalin for histologic analysis. Because repeated handling and injections can cause pain or other adverse effects which would be reflected by a decrease in food intake, the body weight of each mouse was monitored throughout the course of the study. All mice gained weight consistently over the course of the study, and there was no difference in the average body weights of each group at any time point during the study (data not shown).

Histology processing and OA grading. The formalin-fixed mouse hind limbs were transferred to 70% ethanol, and the excess soft tissue was removed. The samples were decalcified in 19% EDTA (Fisher Scientific), and the intact joints were embedded in paraffin. The joints were sectioned along the coronal plane at 4 μm. Mid-coronal sections were stained with hematoxylin and eosin (H&E) and scored using the ACS score developed by McNulty et al (25). This system scores the integrity of the articular cartilage on a scale of 0–12, where 0 represents normal healthy cartilage and 12 represents full-thickness loss of the articular cartilage across more than two-thirds of the surface scored. Adjacent mid-coronal sections were also stained with Safranin O and fast green and scored using the Saf-O score developed by McNulty et al (25). The Saf-O system scores the proteoglycan content of the articular cartilage on a scale of 0–12, where 0 represents uniform staining of healthy cartilage and 12 represents complete loss of staining across more than two-thirds of the surface. The Saf-O score is more sensitive to the mild-to-moderate lesions that result from the DMM procedure, since it relies on proteoglycan loss from the matrix versus fibrillation and loss of cartilage. Therefore, it (rather than the ACS scoring system) was used to score OA in those experiments. Additional joint measurements were made using the OsteoMeasure histomorphometry system (OsteoMetrics) as previously described (25). The additional parameters measured were articular cartilage area and thickness, subchondral bone area and thickness, number of viable chondrocytes, area of chondrocyte necrosis, and calcified cartilage area and thickness.

Osteophyte assessment. Osteophytes were graded using a system that was modified from a previously published study (26). Osteophytes were graded on a scale of 0–3, where 0 = no osteophyte, 1 = questionable/borderline osteophyte, 2 = small osteophyte, and 3 = large osteophyte. The summed osteophyte scores for the medial tibial plateau and the medial femoral condyle are presented.

Synovial assessment. Coronal sections were immunostained with anti-S100A8 (kindly provided by Dr. Johannes Roth, Institute of Immunology, University of Munster, Munster, Germany), which has been used as a method to detect synovitis with synovial hyperplasia in mouse joints with OA (27). Immunohistochemistry was performed as described above except that proteinase K was used for antigen retrieval. Synovial hyperplasia was graded on a single mid-coronal section from each mouse using a scale of 0–3 as follows: 0 = 1–3 cell layers in synovium, 1 = 4–6 cell layers, 2 = 7–9 cell layers, and 3 = 10 or more cell layers. The medial and lateral compartments of the joint were scored separately, and the sum of the 2 scores is presented.

Micro–computed tomography (micro-CT) analysis. The knee joints from 8-week-old male $MIF^{-/-}$ mice and wild-type mice (n = 3 per group) and 12-month-old male $MIF^{-/-}$ mice (n = 4) and wild-type mice (n = 5) were scanned at 10 μm resolution by micro-CT (μct80; Scanco Medical) as previously described (28). Bone morphometric parameters were measured in the trabecular bone of the proximal metaphysis of the tibia using Scanco software. The region of interest was consistently defined to begin inferior to the growth plate and extended for 1.00 mm distally. Bone image data were rotated as necessary to adjust for any vertical alignments. The following histomorphometric trabecular bone parameters (29) were analyzed using the same threshold for each animal: bone volume fraction, tissue mineral density, connectivity density, trabecular number, trabecular separation, and trabecular thickness.

Statistical analysis. All statistical analyses were performed using GraphPad Prism 6 with one exception. OA histomorphometry measurements were analyzed using SPSS, as noted. Data are presented graphically as individual data points with horizontal lines representing the mean of each group. MIF ELISA samples were collected from monolayer cultures of cells or explant cultures from unique human tissue donors (n = 7–16 donors per group) and analyzed by unpaired t-test within each tissue type. OA severity (ACS and Saf-O scores) in individual mice (n = 13–16 mice per group) was analyzed by Kruskal-Wallis nonparametric one-way analysis of variance (ANOVA) followed by Dunn's multiple comparison test. Histomorphometric measurements were analyzed by heteroscedastic t-test. Synovial hyperplasia was evaluated in a subset of mice from the 12-month-old and 22-month-old groups (n = 5–11 mice per group) and analyzed by Kruskal-Wallis nonparametric one-way ANOVA followed by Dunn's multiple comparison test. Bone parameters were measured in individual mice (n = 3–5 mice per group) and analyzed by two-way ANOVA followed by Tukey's multiple comparison post hoc test.

RESULTS

Secretion of higher levels of MIF by human OA chondrocytes than normal chondrocytes. Due to previously published results showing that MIF is present at higher levels in OA synovial fluid than in normal synovial
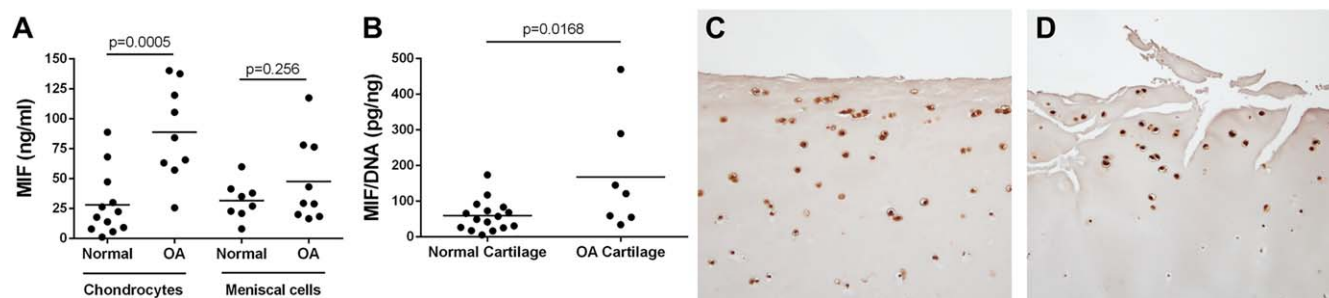
Figure 1. Macrophage migration inhibitory factor (MIF) levels in conditioned media from normal and osteoarthritic (OA) human chondrocyte and meniscal cell cultures and in normal and OA human cartilage sections. **A,** MIF levels in normal and OA chondrocytes and meniscal cells. Serum-free medium was collected after 16 hours of culture from unstimulated confluent monolayers of normal and OA chondrocytes and meniscal cells. MIF protein in media was measured by human MIF enzyme-linked immunosorbent assay (ELISA). Circles represent individual samples; horizontal lines show the mean (n = 12 donors for normal chondrocytes, 9 donors for OA chondrocytes, 8 donors for normal meniscus, and 9 donors for OA meniscus). *P* values were determined by unpaired *t*-test. **B,** MIF levels in normal and OA cartilage. Serum-free conditioned medium was collected after 48 hours of culture from unstimulated normal and OA cartilage explants. MIF protein in media was measured by human MIF ELISA and was normalized to the DNA content of the explants. Circles represent individual samples; horizontal lines show the mean (n = 16 donors for normal cartilage explants and 7 donors for OA cartilage explants). *P* values were determined by unpaired *t*-test. No outliers were identified by the Grubbs outlier test. **C** and **D,** Immunohistochemistry results for MIF in sections of normal (**C**) and OA (**D**) human knee cartilage.

fluid (14,18), the amount of MIF secreted by joint tissue cells was measured to determine which tissues could be a source of MIF within the joint. Conditioned media samples were collected from unstimulated monolayer cultures of chondrocytes and meniscal cells and from unstimulated cartilage explant cultures, and the MIF protein level in the media was measured by ELISA (Figures 1A and B). Chondrocytes isolated from OA cartilage secreted a mean ± SD of 88.76 ± 13.14 ng/ml of MIF over 16 hours, which was significantly higher ($P = 0.0005$) than that produced by chondrocytes from normal cartilage, which secreted a mean ± SD of 28.23 ± 7.78 ng/ml of MIF. Cells from OA meniscus secreted a mean ± SD of 47.62 ± 11.73 ng/ml of MIF, which was not significantly different from cells isolated from normal meniscus (31.65 ± 5.54 ng/ml). MIF in conditioned media from OA synovial fibroblasts was not detectable (data not shown).

OA cartilage explants released a mean ± SD of 167.9 ± 55.92 pg MIF/ng DNA, which was significantly higher ($P = 0.0168$) than that produced by normal cartilage explants, which released a mean ± SD of 59.21 ± 10.87 pg MIF/ng DNA. MIF levels in human cartilage were visualized by immunostaining. MIF was localized to chondrocytes in sections from both normal donors (Figure 1C) and OA donors (Figure 1D) without significant differences in immunopositivity, suggesting that the differences noted in cultured cells and explants were due to differences in MIF release into the media.

Reduced severity of naturally occurring OA with age in mice with MIF deletion. In order to determine if MIF contributes to the development of OA in vivo, the knee joints from 12-month-old and 22-month-old male

MIF$^{-/-}$ and wild-type mice were analyzed for OA severity. Histologic evaluation of H&E-stained sections revealed characteristic OA changes in the joints of the wild-type mice at both ages, including degradation and loss of the articular cartilage, thickening of the subchondral bone, and osteophyte formation (Figure 2A). In contrast, the joints of the MIF$^{-/-}$ mice displayed more healthy appearing articular cartilage, normal thickness of the subchondral bone, and no osteophyte formation. Anti-MIF immunostaining in a wild-type mouse section showed MIF expression in the meniscus and the articular cartilage (Figure 2A). As expected, there was a lack of staining for MIF in the sections from MIF$^{-/-}$ mice.

OA severity, graded using the ACS score, was significantly higher in the wild-type relative to the MIF$^{-/-}$ mice at both 12 and 22 months of age (Figure 2B). Wild-type mice at 12 and 22 months developed significantly larger osteophytes than the MIF$^{-/-}$ mice (Figure 2C). The joints of the 12-month-old and 22-month-old MIF$^{-/-}$ and wild-type mice were further evaluated using histomorphometric analysis (Table 1). In both age groups, the MIF$^{-/-}$ mice maintained significantly greater articular cartilage area and thickness and more viable chondrocytes than the wild-type mice. Subchondral bone changes were also evident between the genotypes. The subchondral bone area and thickness were significantly greater in wild-type mice than in MIF$^{-/-}$ mice. The only 2 parameters that were not significantly different between MIF$^{-/-}$ and wild-type mice were the area of chondrocyte necrosis and the calcified cartilage area.

Synovitis with synovial hyperplasia is another characteristic of OA. S100A8 is an alarmin protein that is produced by synovial cells as well as activated macrophages and has
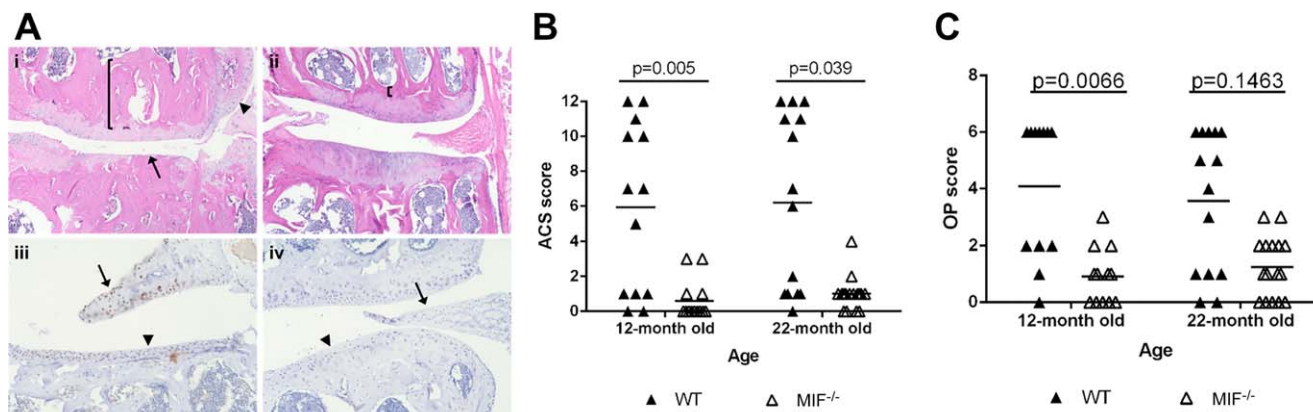
Figure 2. Mice with macrophage migration inhibitory factor (MIF) deletion are protected against age-related osteoarthritis (OA). **A,** Representative histologic images of knee joint sections in 12-month-old MIF$^{-/-}$ and wild-type (WT) mice. **i,** Hematoxylin and eosin (H&E)–stained section of the medial tibial plateau of a wild-type mouse with an articular cartilage structure (ACS) score of 11. **Arrow** indicates degradation and loss of articular cartilage; **arrowhead** indicates osteophyte formation; **bracket** indicates thickening of subchondral bone. **ii,** H&E-stained section from an MIF$^{-/-}$ mouse with an ACS score of 3. **Bracket** indicates normal subchondral bone thickness. **iii,** Wild-type mouse section immunostained for MIF. Intracellular MIF is present in the meniscus (**arrow**) and articular cartilage (**arrowhead**). **iv,** MIF$^{-/-}$ mouse section immunostained for MIF, showing a lack of MIF immunopositivity in the meniscus (**arrow**) and cartilage (**arrowhead**). **B** and **C,** ACS score (**B**) and osteophyte (OP) score (**C**) in MIF$^{-/-}$ and wild-type mice. The medial tibial plateau of mid-coronal knee sections was scored using the ACS score. Osteophyte scores are the sum of the scores for the medial tibial plateau and the medial femoral condyle. Symbols represent individual mice; horizontal lines show the mean (n = 13 12-month-old wild-type mice, 13 12-month-old MIF$^{-/-}$ mice, 14 22-month-old wild-type mice, and 16 22-month-old MIF$^{-/-}$ mice). *P* values were determined by Kruskal-Wallis nonparametric one-way analysis of variance followed by Dunn's multiple comparison test.

been shown to correlate with synovitis (27,30). Here, immunohistochemistry was performed using anti-S100A8 on coronal sections from 12-month-old and 22-month-old wild-type and MIF$^{-/-}$ mice (representative images are shown in Figures 3A and B). In both genotypes, immunopositivity was evident throughout the joint—in the articular cartilage, the meniscus, and the synovium. Specifically in the wild-type mouse joints, S100A8 immunopositivity was strong in both the cells and matrix of the synovium. As

shown in Figure 3A, S100A8 immunopositivity correlated with areas of synovial hyperplasia and thickening of the synovial lining. In contrast, S100A8 synovial immunostaining revealed minimal synovial hyperplasia in the MIF$^{-/-}$ mice. Based on the synovial scoring system described above, there was no difference in synovial hyperplasia between the 12-month-old wild-type and MIF$^{-/-}$ mice, while the 22-month-old wild-type mice exhibited more severe synovial hyperplasia than the 22-month-old MIF$^{-/-}$

Table 1. Histomorphometric analysis of aged mice with macrophage migration inhibitory factor deletion and wild-type controls*

Parameter	12-month-old mice			22-month-old mice			
	MIF$^{-/-}$ (n = 13)	Wild-type (n = 13)	*P*†	MIF$^{-/-}$ (n = 16)	Wild-type (n = 14)	*P*†	*P*‡
Articular cartilage area, mm^2	0.064 ± 0.011	0.040 ± 0.016	<0.001	0.064 ± 0.008	0.029 ± 0.018	<0.001	0.089
Articular cartilage thickness, mm	0.072 ± 0.013	0.043 ± 0.017	<0.001	0.078 ± 0.009	0.037 ± 0.019	<0.001	0.339
Subchondral bone area, mm^2	0.080 ± 0.016	0.156 ± 0.069	0.002	0.070 ± 0.025	0.103 ± 0.038	0.009	0.024
Subchondral bone thickness, mm	0.059 ± 0.011	0.104 ± 0.046	0.004	0.070 ± 0.023	0.100 ± 0.037	0.013	0.772
Number of viable chondrocytes	138.39 ± 16.15	74.31 ± 41.38	<0.001	115.50 ± 21.98	64.14 ± 45.24	0.001	0.549
Area of chondrocyte necrosis, mm^2	0.008 ± 0.006	0.006 ± 0.004	0.396	0.008 ± 0.011	0.007 ± 0.008	0.859	0.602
Calcified cartilage area, mm^2	0.063 ± 0.012	0.059 ± 0.019	0.504	0.049 ± 0.005	0.053 ± 0.019	0.368	0.421

* Values are the mean ± SD. Histomorphometric measurements of cartilage and bone parameters in the medial tibial compartment of mid-coronal mouse knee sections were analyzed using the Osteomeasure Histomorphometry Program (OsteoMetrics).
† By heteroscedastic *t*-test using SPSS.
‡ Twelve-month-old wild-type mice versus 22-month-old wild-type mice, by heteroscedastic *t*-test using SPSS.
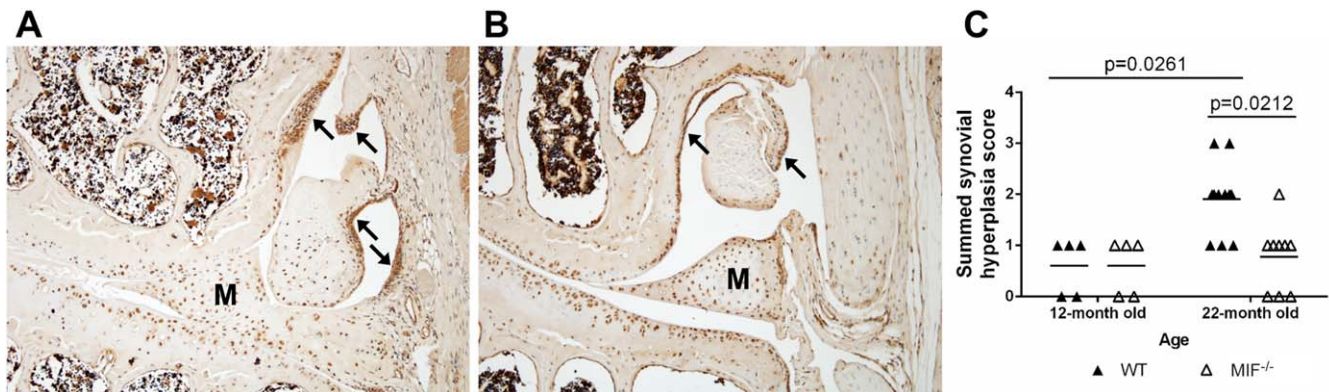
Figure 3. Reduced severity of synovial hyperplasia in 22-month-old mice with macrophage migration inhibitory factor (MIF) deletion. **A** and **B,** Immunohistochemistry results for S100A8 in sections from a 22-month-old wild-type (WT) mouse with an articular cartilage structure (ACS) score of 11 (**A**) and a 22-month-old MIF$^{-/-}$ mouse with an ACS score of 0 (**B**). Representative histologic images are shown. **Arrows** indicate regions of strong synovial S100A8 immunopositivity and synovial hyperplasia. **M** = meniscus. **C,** Sum of the synovial hyperplasia scores of the medial and lateral compartments in wild-type and MIF$^{-/-}$ mice. Symbols represent individual mice; horizontal lines show the mean (n = 5 12-month-old wild-type mice, 5 12-month-old MIF$^{-/-}$ mice, 11 22-month-old wild-type mice, and 9 22-month-old MIF$^{-/-}$ mice). *P* values were determined by Kruskal-Wallis nonparametric one-way analysis of variance followed by Dunn's multiple comparison test.

mice (Figure 3C). Additionally, the severity of synovial hyperplasia increased between 12 and 22 months in the wild-type mice.

Early bone differences in mice with MIF deletion are not maintained with age. Because of conflicting reports of bone density differences in MIF$^{-/-}$ mice compared to

wild-type mice (31,32) and the possibility that bone density differences could influence the development of OA (33), we measured trabecular bone parameters by micro-CT scans of the proximal metaphysis of the tibia from 8-week-old and 12-month-old male MIF$^{-/-}$ and wild-type mice. The 8-week-old male MIF$^{-/-}$ mice had significantly greater bone
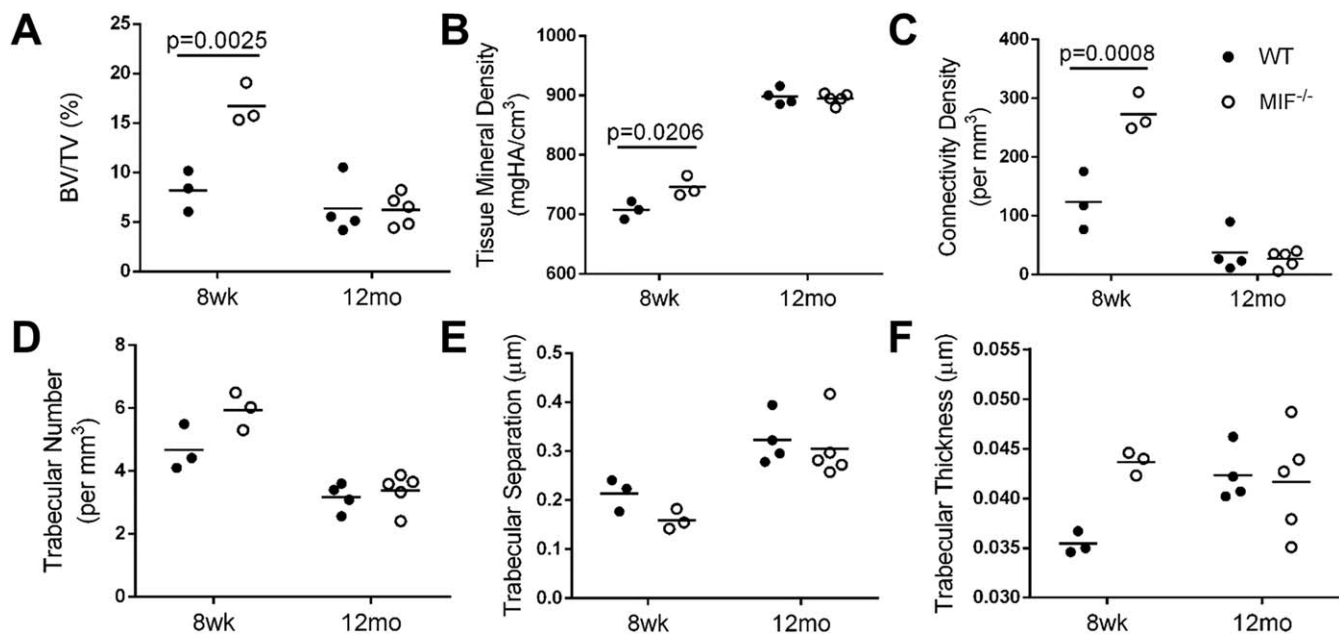
Figure 4. Micro–computed tomography analysis of 8-week-old and 12-month-old male mice with macrophage migration inhibitory factor (MIF) deletion and wild-type (WT) controls. Bone density parameters in the proximal metaphysis of the tibia were analyzed using Scanco software. **A,** Bone volume/total volume (BV/TV). **B,** Tissue mineral density. HA = hydroxyapatite. **C,** Connectivity density. **D,** Trabecular number. **E,** Trabecular separation. **F,** Trabecular thickness. Symbols represent individual mice; horizontal lines show the mean (n = 3 8-week-old wild-type mice, 3 8-week-old MIF$^{-/-}$ mice, 4 12-month-old wild-type mice, and 5 12-month-old MIF$^{-/-}$ mice). *P* values were determined by two-way analysis of variance followed by Tukey's multiple comparison post hoc test.
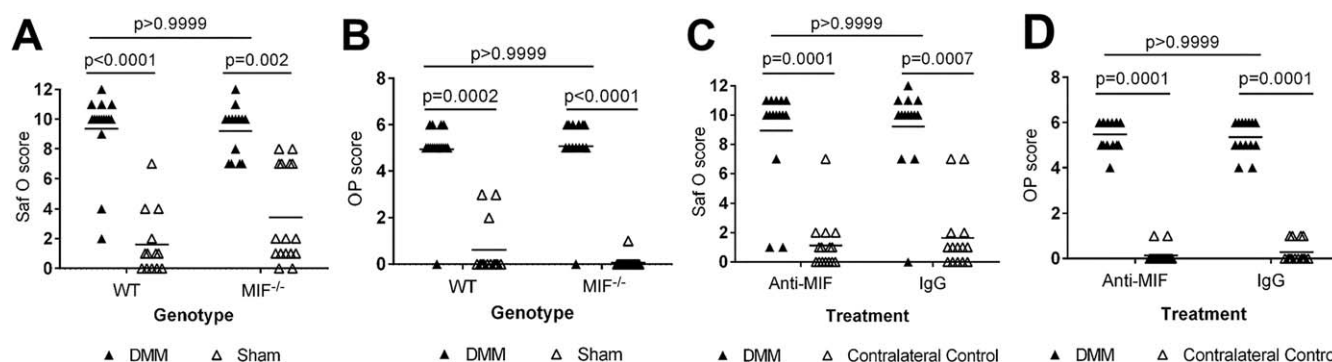
Figure 5. Inhibition of macrophage migration inhibitory factor (MIF) activity either by gene deletion or by neutralizing antibody does not protect young adult mice against injury-induced osteoarthritis (OA). **A** and **B,** Saf-O score, indicating OA severity 10 weeks after surgery (**A**) and sum of the osteophyte (OP) scores in the medial tibial plateau and medial femoral condyle (**B**) in 12-week-old wild-type (WT) and MIF$^{-/-}$ mice subjected to either destabilization of the medial meniscus (DMM) or sham surgery. Symbols represent individual mice; horizontal lines show the mean (n = 14 MIF$^{-/-}$ mice with DMM, 16 sham-operated MIF$^{-/-}$ mice, 16 wild-type mice with DMM, and 13 sham-operated wild-type mice). **C** and **D,** Saf-O score, indicating OA severity 10 weeks after surgery (**C**) and sum of the osteophyte scores in the medial tibial plateau and medial femoral condyle (**D**) in 12-week-old wild-type mice subjected to DMM and treated for 10 weeks with either MIF-neutralizing antibody (anti-MIF) or IgG control antibody. The contralateral limb was used as the unoperated control. Symbols represent individual mouse limbs; horizontal lines show the mean (n = 15 limbs with DMM from mice treated with anti-MIF, 15 contralateral control limbs from mice treated with anti-MIF, 14 limbs with DMM from mice treated with IgG, and 14 contralateral control limbs from mice treated with IgG). *P* values were determined by Kruskal-Wallis nonparametric one-way analysis of variance followed by Dunn's multiple comparison test.

volume fraction (Figure 4A), tissue mineral density (Figure 4B), and connectivity density (Figure 4C) than the age-matched wild-type mice. These differences were not maintained with age, as there were no significant differences in any bone parameters between 12-month-old male MIF$^{-/-}$ and wild-type mice. Bone density parameters were also measured in female mice of the same ages, but there were no differences in these parameters between MIF$^{-/-}$ and wild-type mice in either age group (data not shown).

MIF deletion or treatment with an MIF-neutralizing antibody does not reduce the severity of surgically induced OA in young adult mice. We next wanted to determine if MIF was required for the development of surgically induced OA in young adult mice. We used the DMM surgical model to induce OA in 12-week-old male MIF$^{-/-}$ and wild-type mice and evaluated the severity of cartilage lesions 10 weeks after surgery. Compared to the sham-operated controls, both the wild-type mice and MIF$^{-/-}$ mice developed significant cartilage lesions; however, in contrast to the data on natural age-related OA, there was no difference in severity between the 2 groups (Figure 5A). Both the wild-type mice and MIF$^{-/-}$ mice subjected to DMM developed significantly larger osteophytes than the sham-operated mice, but there was no difference between the 2 groups (Figure 5B).

We also determined if inhibition of MIF systemically, using a neutralizing antibody, would alter the severity of surgically induced OA. Twelve-week-old male C57BL/6 mice underwent the DMM procedure and were then treated for 10 weeks with either an MIF-neutralizing

antibody or an IgG control antibody. The dose of anti-MIF used here was sufficient to inhibit MIF activity in a previous study (24). OA severity was analyzed 10 weeks after surgery (Figure 5C). Due to limitations in the amount of MIF antibody available and our previous data indicating that a sham-operated control group did not develop OA changes, the contralateral legs were scored as the control group in this study. The limbs of the mice in the control IgG-treated group and the anti-MIF–treated group subjected to DMM developed significantly more severe OA than the contralateral limbs, and there was no difference in OA severity between the 2 treatment groups. The limbs of the mice in both the IgG and MIF treatment groups subjected to DMM developed significantly larger osteophytes than the contralateral limbs (Figure 5D).

DISCUSSION

Although OA is characterized by common pathologic changes within affected joints, the pathways that lead to OA can vary depending on the inciting factors. In this study, we demonstrated that deletion of the proinflammatory cytokine MIF protects mice against developing naturally occurring age-related OA but not against developing injury-induced OA. These findings are in stark contrast to previous studies of mice with deletion of the proinflammatory cytokine IL-6, where age-related OA was more severe in the IL-6–knockout mice (34), while they were protected against injury-induced OA in the same DMM model used in the present study (35). Other studies have also shown

different effects when age-related and injury-induced OA were evaluated in mice with specific gene deletions, including MMP-3 deletion which, similar to our findings, resulted in less severe age-related OA but had no effect on OA severity in an injury model (for review, see ref. 36). These studies emphasize the need to consider more than one model of OA when determining the role of a particular factor and indicate that the successful treatment of age-related OA and posttraumatic OA may require different targets.

The aged MIF-knockout mouse not only exhibited less articular cartilage damage compared to age-matched wild-type mice but also less synovial hyperplasia and fewer OA bone changes, including osteophytes. Synovial inflammation is evident in >60% of clinical cases of OA as measured by magnetic resonance imaging (37). Synovial inflammation is a key source of pain in OA due to macrophage infiltration and increased vascularization and innervation of the synovium (38). We used the alarmin S100A8 as a marker of synovial changes due to its strong correlation with synovial hyperplasia and synovitis as well as its association with macrophage infiltration in the synovium (27,30). However, while there is a clear correlation between the MIF genotype, synovial hyperplasia, and OA severity, it is difficult to determine if lack of MIF resulted in less synovial involvement and this contributed to cartilage protection or if less cartilage damage in the $MIF^{-/-}$ mice resulted in less synovial hyperplasia.

The DMM model effectively induces OA changes in the cartilage and bone, but minimal synovitis has been observed in this model (39). We also did not observe significant synovitis or synovial hyperplasia in mice subjected to DMM (data not shown), suggesting that the differential effect of MIF-knockout on age-related OA and DMM-induced OA may be due to a differential role of the synovium. This would be consistent with studies that have shown that MIF contributes to synovitis in models of inflammatory arthritis (40). Since MIF is constitutively expressed in the joint, it is possible that it exerts an age-related deleterious action on joint homeostasis but is not important in the acute setting of joint injury when the expression of other inflammatory mediators prevails.

The finding that the ACS scores in the wild-type mice did not change significantly between 12 and 22 months was unexpected. Since this was a cross-sectional study, it is not possible to determine if this was due to a lack of progression of the cartilage changes or just a chance occurrence in two different sets of mice. However, we did note that there was a significant decrease in the subchondral bone area between the 12-month-old and 22-month-old wild-type mice, and there was a trend toward a significant decrease in the articular cartilage area between

the 2 groups, but we did not note differences in the number of viable chondrocytes or in the area of chondrocyte necrosis. These aging changes in the mice are similar to aging changes in humans where there is a thinning of the articular cartilage (2), a decrease in the number of viable chondrocytes (41), and an overall increase in bone turnover (1).

There is some controversy over the role of MIF in bone. Studies have shown that MIF inhibits osteoclastogenesis through activation of the tyrosine kinase Lyn (42), and that $MIF^{-/-}$ mice have significantly less bone volume than wild-type mice (32). Alternatively, MIF has been shown to be necessary for osteoclastogenesis in a mouse model of RA, and $MIF^{-/-}$ mice were protected against development of bone erosions in this model (15). Because increased bone density has been shown to be a potential risk factor for incident OA, while increased bone turnover may promote progression (43,44), we examined bone density in young and older adult $MIF^{-/-}$ mice. We found that the bone volume fraction and other bone parameters were higher in young $MIF^{-/-}$ mice compared to wild-type mice, but these early bone differences were not maintained with age. Therefore, it is unlikely that these early bone density differences were responsible for the reduced OA severity seen in the older adult $MIF^{-/-}$ mice.

It is not clear from the present study if MIF deletion had a direct effect on the articular chondrocytes that could explain less severe age-related OA. Immuno-histochemistry results revealed that chondrocytes, as well as meniscal cells, were immunopositive for MIF and released MIF into the media when cultured. Similar intracellular staining and release has been seen with other cell types such as macrophages (12) and RA synovial fibroblasts (14). Chondrocytes, but not meniscal cells, from OA joints secreted more MIF than cells from normal joints. However, we could not detect an effect of extracellular MIF on joint tissue cells. We performed a series of in vitro studies using recombinant MIF in doses of up to 1 μg/ml and could not detect an increase in ERK, p38, or JNK MAP kinase activation or increase in MMP production in cultures of human chondrocytes, meniscal cells, or synovial fibroblasts (see Supplementary Figure 1, available on the *Arthritis & Rheumatology* web site at http://onlinelibrary.wiley.com/doi/10.1002/art.39844/abstract).

These in vitro results in joint tissue cells are contrary to the findings of published studies with other cell types that showed recombinant MIF–stimulated phosphorylation of the ERK MAP kinase in Raji cells (a B cell line) (9) and in primary rat osteoblasts (45). Additional published studies show recombinant MIF-stimulated production of MMP-1 and MMP-3 in

synovial fibroblasts isolated from OA and RA patients (13) as well as MMP-9 and MMP-13 production in primary rat osteoblasts (45). However, those studies required doses of MIF of up to 10 μg/ml to detect a response, which far exceeds the amount of MIF measured in synovial fluid, which ranges from 3 to 19 ng/ml (14,18), or the amount of MIF we measured in conditioned media from confluent chondrocyte and meniscal cell monolayers, which ranged from 1 to 140 ng/ml. We examined chondrocytes for the presence of CD74, which is the primary receptor for MIF, but could not detect significant levels on the cell surface by flow cytometry (Rowe MA, et al: unpublished observations).

These findings suggest that chondrocytes produce and secrete MIF but that it does not have an autocrine effect on cartilage. MIF may instead promote OA by promoting macrophage infiltration into the joint, which would explain the reduced synovial hyperplasia observed in the aged mice with MIF deleted. MIF also has been described to exert intracellular functions by intracytoplasmic interaction with the COP9 signalosome that influences cell cycle progression (46). Accordingly, the distinction we observed between the effects of MIF deletion versus immunoneutralization may be accounted for by a strictly intracellular role for MIF in chondrocytes.

Taken together, our findings indicate that the lack of MIF has a strong protective effect on naturally occurring age-related OA. As the percentage of adults older than 65 continues to increase, the prevalence of aging-related diseases, including OA, is also increasing (47). MIF is encoded in a functionally polymorphic locus that occurs commonly in the population (48), and our data prompt investigation into the potential role of variant MIF alleles in OA incidence or progression. Therapies that are able to stop or slow the progression of diseases of aging are necessary in order to improve the quality of life and to extend the healthy lifespan of the aging population.

REFERENCES

1. Loeser RF. Age-related changes in the musculoskeletal system and the development of osteoarthritis. Clin Geriatr Med 2010; 26:371–86.
2. Ding C, Cicuttini F, Scott F, Cooley H, Jones G. Association between age and knee structural change: a cross sectional MRI based study. Ann Rheum Dis 2005;64:549–55.
3. Chen AC, Temple MM, Ng DM, Verzijl N, DeGroot J, TeKoppele JM, et al. Induction of advanced glycation end products and alterations of the tensile properties of articular cartilage. Arthritis Rheum 2002;46:3212–7.
4. Loeser RF, Gandhi U, Long DL, Yin W, Chubinskaya S. Aging and oxidative stress reduce the response of human articular chondrocytes to insulin-like growth factor 1 and osteogenic protein 1. Arthritis Rheumatol 2014;66:2201–9.
5. Messai H, Duchossoy Y, Khatib AM, Panasyuk A, Mitrovic DR. Articular chondrocytes from aging rats respond poorly to insulin-like growth factor-1: an altered signaling pathway. Mech Ageing Dev 2000;115:21–37.
6. Blaney Davidson EN, Scharstuhl A, Vitters EL, van der Kraan PM, van den Berg WB. Reduced transforming growth factor-β signaling in cartilage of old mice: role in impaired repair capacity. Arthritis Res Ther 2005;7:R1338–47.
7. Bobacz K, Gruber R, Soleiman A, Erlacher L, Smolen JS, Graninger WB. Expression of bone morphogenetic protein 6 in healthy and osteoarthritic human articular chondrocytes and stimulation of matrix synthesis in vitro. Arthritis Rheum 2003;48: 2501–8.
8. Greene MA, Loeser RF. Aging-related inflammation in osteoarthritis. Osteoarthritis Cartilage 2015;23:1966–71.
9. Leng L, Metz CN, Fang Y, Xu J, Donnelly S, Baugh J, et al. MIF signal transduction initiated by binding to CD74. J Exp Med 2003;197:1467–76.
10. Rajasekaran D, Zierow S, Syed M, Bucala R, Bhandari V, Lolis EJ. Targeting distinct tautomerase sites of D-DT and MIF with a single molecule for inhibition of neutrophil lung recruitment. FASEB J 2014;28:4961–71.
11. Mitchell RA, Liao H, Chesney J, Fingerle-Rowson G, Baugh J, David J, et al. Macrophage migration inhibitory factor (MIF) sustains macrophage proinflammatory function by inhibiting p53: regulatory role in the innate immune response. Proc Natl Acad Sci U S A 2002;99:345–50.
12. Calandra T, Bernhagen J, Mitchell RA, Bucala R. The macrophage is an important and previously unrecognized source of macrophage migration inhibitory factor. J Exp Med 1994;179:1895–902.

13. Onodera S, Kaneda K, Mizue Y, Koyama Y, Fujinaga M, Nishihira J. Macrophage migration inhibitory factor up-regulates expression of matrix metalloproteinases in synovial fibroblasts of rheumatoid arthritis. J Biol Chem 2000;275:444–50.

14. Onodera S, Tanji H, Suzuki K, Kaneda K, Mizue Y, Sagawa A, et al. High expression of macrophage migration inhibitory factor in the synovial tissues of rheumatoid joints. Cytokine 1999;11:163–7.

15. Gu R, Santos LL, Ngo D, Fan H, Singh PP, Fingerle-Rowson G, et al. Macrophage migration inhibitory factor is essential for osteoclastogenic mechanisms in vitro and in vivo mouse model of arthritis. Cytokine 2015;72:135–45.

16. Foote A, Briganti EM, Kipen Y, Santos L, Leech M, Morand EF. Macrophage migration inhibitory factor in systemic lupus erythematosus. J Rheumatol 2004;31:268–73.

17. Hoi AY, Hickey MJ, Hall P, Yamana J, O'Sullivan KM, Santos LL, et al. Macrophage migration inhibitory factor deficiency attenuates macrophage recruitment, glomerulonephritis, and lethality in MRL/lpr mice. J Immunol 2006;177:5687–96.

18. Liu M, Hu C. Association of MIF in serum and synovial fluid with severity of knee osteoarthritis. Clin Biochem 2012;45:737–9.

19. Harper JM, Wilkinson JE, Miller RA. Macrophage migration inhibitory factor-knockout mice are long lived and respond to caloric restriction. FASEB J 2010;24:2436–42.

20. Bernhagen J, Krohn R, Lue H, Gregory JL, Zernecke A, Koenen RR, et al. MIF is a noncognate ligand of CXC chemokine receptors in inflammatory and atherogenic cell recruitment. Nat Med 2007;13:587–96.

21. Loeser RF, Pacione CA, Chubinskaya S. The combination of insulin-like growth factor 1 and osteogenic protein 1 promotes increased survival of and matrix synthesis by normal and osteoarthritic human articular chondrocytes. Arthritis Rheumatol 2003;48:2188–96.

22. Yin W, Park JI, Loeser RF. Oxidative stress inhibits insulin-like growth factor-I induction of chondrocyte proteoglycan synthesis through differential regulation of phosphatidylinositol 3-Kinase-Akt and MEK-ERK MAPK signaling pathways. J Biol Chem 2009;284:31972–31981.

23. Loeser RF, Olex AL, McNulty MA, Carlson CS, Callahan MF, Ferguson CM, et al. Microarray analysis reveals age-related differences in gene expression during the development of osteoarthritis in mice. Arthritis Rheum 2012;64:705–17.

24. Leng L, Chen L, Fan J, Greven D, Arjona A, Du X, et al. A small-molecule macrophage migration inhibitory factor antagonist protects against glomerulonephritis in lupus-prone NZB/ NZW F1 and MRL/lpr mice. J Immunol 2011;186:527–38.

25. McNulty MA, Loeser RF, Davey C, Callahan MF, Ferguson CM, Carlson CS. A comprehensive histological assessment of osteoarthritis lesions in mice. Cartilage 2011;2:354–63.

26. Miller RE, Tran PB, Das R, Ghoreishi-Haack N, Ren D, Miller RJ, et al. CCR2 chemokine receptor signaling mediates pain in experimental osteoarthritis. Proc Natl Acad Sci U S A 2012;109:20602–7.

27. Schelbergen RF, de Munter W, van den Bosch MH, Lafeber FP, Sloetjes A, Vogl T, et al. Alarmins S100A8/S100A9 aggravate osteophyte formation in experimental osteoarthritis and predict osteophyte progression in early human symptomatic osteoarthritis. Ann Rheum Dis 2016;75:218–25.

28. Lau AG, Sun J, Hannah WB, Livingston EW, Heymann D, Bateman TA, et al. Joint bleeding in factor VIII deficient mice causes an acute loss of trabecular bone and calcification of joint soft tissues which is prevented with aggressive factor replacement. Haemophilia 2014;20:716–22.

29. Muller R, van Campenhout H, van Damme B, van der Perre G, Dequeker J, Hildebrand T, et al. Morphometric analysis of human bone biopsies: a quantitative structural comparison of histological sections and micro-computed tomography. Bone 1998;23:59–66.

30. Schelbergen RF, van Dalen S, ter Huurne M, Roth J, Vogl T, Noel D, et al. Treatment efficacy of adipose-derived stem cells in experimental osteoarthritis is driven by high synovial activation and reflected by S100A8/A9 serum levels. Osteoarthritis Cartilage 2014;22:1158–66.

31. Oshima S, Onodera S, Amizuka N, Li M, Irie K, Watanabe S, et al. Macrophage migration inhibitory factor-deficient mice are resistant to ovariectomy-induced bone loss. FEBS Lett 2006;580: 1251–6.

32. Jacquin C, Koczon-Jaremko B, Aguila HL, Leng L, Bucala R, Kuchel GA, et al. Macrophage migration inhibitory factor inhibits osteoclastogenesis. Bone 2009;45:640–9.

33. Hardcastle SA, Dieppe P, Gregson CL, Davey Smith G, Tobias JH. Osteoarthritis and bone mineral density: are strong bones bad for joints? Bonekey Rep 2015;4:624.

34. De Hooge AS, van de Loo FA, Bennink MB, Arntz OJ, de Hooge P, van den Berg WB. Male IL-6 gene knock out mice developed more advanced osteoarthritis upon aging. Osteoarthritis Cartilage 2005;13:66–73.

35. Ryu JH, Yang S, Shin Y, Rhee J, Chun CH, Chun JS. Interleukin-6 plays an essential role in hypoxia-inducible factor 2α–induced experimental osteoarthritic cartilage destruction in mice. Arthritis Rheum 2011;63:2732–43.

36. Little CB, Zaki S. What constitutes an "animal model of osteoarthritis" – the need for consensus? Osteoarthritis Cartilage 2012;20:261–7.

37. Wang X, Jin X, Han W, Cao Y, Halliday A, Blizzard L, et al. Cross-sectional and longitudinal associations between knee joint effusion synovitis and knee pain in older adults. J Rheumatol 2016;43:121–30.

38. Benito MJ, Veale DJ, FitzGerald O, van den Berg WB, Bresnihan B. Synovial tissue inflammation in early and late osteoarthritis. Ann Rheum Dis 2005;64:1263–7.

39. Jackson MT, Moradi B, Zaki S, Smith MM, McCracken S, Smith SM, et al. Depletion of protease-activated receptor 2 but not protease-activated receptor 1 may confer protection against osteoarthritis in mice through extracartilaginous mechanisms. Arthritis Rheumatol 2014;66:3337–48.

40. Morand EF, Bucala R, Leech M. Macrophage migration inhibitory factor: an emerging therapeutic target in rheumatoid arthritis. Arthritis Rheum 2003;48:291–9.

41. Kuhn K, D'Lima DD, Hashimoto S, Lotz M. Cell death in cartilage. Osteoarthritis Cartilage 2004;12:1–16.

42. Mun SH, Oh D, Lee SK. Macrophage migration inhibitory factor down-regulates the RANKL–RANK signaling pathway by activating Lyn tyrosine kinase in mouse models. Arthritis Rheumatol 2014;66:2482–93.

43. Dequeker J, Aerssens J, Luyten FP. Osteoarthritis and osteoporosis: clinical and research evidence of inverse relationship. Aging Clin Exp Res 2003;15:426–39.

44. Zhang Y, Hannan MT, Chaisson CE, McAlindon TE, Evans SR, Aliabadi P, et al. Bone mineral density and risk of incident and progressive radiographic knee osteoarthritis in women: the Framingham Study. J Rheumatol 2000;27:1032–7.

45. Onodera S, Nishihira J, Iwabuchi K, Koyama Y, Yoshida K, Tanaka S, et al. Macrophage migration inhibitory factor up-regulates matrix metalloproteinase-9 and -13 in rat osteoblasts: relevance to intracellular signaling pathways. J Biol Chem 2002;277:7865–74.

46. Kleemann R, Hausser A, Geiger G, Mischke R, Burger-Kentischer A, Flieger O, et al. Intracellular action of the cytokine MIF to modulate AP-1 activity and the cell cycle through Jab1. Nature 2000;408:211–6.

47. Cross M, Smith E, Hoy D, Nolte S, Ackerman I, Fransen M, et al. The global burden of hip and knee osteoarthritis: estimates from the global burden of disease 2010 study. Ann Rheum Dis 2014;73:1323–30.

48. Bucala R. MIF, MIF alleles, and prospects for therapeutic intervention in autoimmunity. J Clin Immunol 2013;33 Suppl 1:S72–8.